Directional Processing of Color Images: Theory and Experimental Results

Panos E. Trahanias, *Member, IEEE*, Damianos Karakos, and Anastasios N. Venetsanopoulos, *Fellow, IEEE*

***Abstract*—The processing of color image data using directional information is studied in this paper. The class of vector directional filters (VDF), which was introduced by the authors in a previous work, is further considered. The analogy of VDF to the *spherical median* is shown, and their relation to the *spatial median* is examined. Moreover, their statistical and deterministic properties are studied, which demonstrate their appropriateness in image processing. VDF result in optimal estimates of the image vectors in the directional sense; this is very important in the case of color images, where the vectors' direction signifies the chromaticity of a given color. Issues regarding the practical implementation of VDF are also considered. In addition, efficient filtering schemes based on VDF are proposed, which include adaptive and/or double-window structures.**

Experimental and comparative results in image filtering show very good performance measures when the error is measured in the $L^*a^*b^*$ space. $L^*a^*b^*$ is known as a space where equal color differences result in equal distances, and therefore, it is very close to the human perception of colors. Moreover, an indication of the chromaticity error is obtained by measuring the error on the Maxwell triangle; the results demonstrate that VDF are very accurate chromaticity estimators.

I. Introduction

COLOR image data processing is studied in this paper using a vector approach [2]. The value at each image pixel is taken to be a 3-D vector, and the processing approach considers the direction of the image vectors and their magnitudes. The class of vector directional filters (VDF), which was previously introduced by the authors [1], is further developed and studied in this paper from a theoretical and an applications point of view. It is shown that the VDF can actually be derived as directional estimates on spherical data [3]. More specifically, the VDF direction is the spherical median [4] with the added constraint that the filter output be one of the inputs. Consequently, VDF operate optimally in the sense of direction preservation. This is very important in color image processing since the direction of the vectors signifies the color chromaticity. As a result, VDF operate as chromaticity preserving filters.

Manuscript received November 15, 1994; revised December 11, 1995.

P. E. Trahanias is with the Institute of Computer Science, Foundation for Research, and Technology, Heraklion, Crete, Greece and the Department of Computer Science, University of Crete, Heraklion, Crete, Greece.

D. Karakos was with the Institute of Computer Science, Foundation for Research, and Technology, Heraklion, Crete, Greece, and the Department of Computer Science, University of Crete, Heraklion, Crete, Greece. He is now with the Institute for Systems Research, University of Maryland at College Park, College Park, MD 20742 USA.

A. N. Venetsanopoulos is with the Department of Electrical and Computer Engineering, University of Toronto, Toronto, Canada M5S 1A4.

Publisher Item Identifier S 1057-7149(96)04188-7.

Color image processing has traditionally been approached in a component-wise manner, i.e., the image channels are processed separately [5]–[7]. However, these approaches fail to consider the inherent correlation that exists between the different channels. Moreover, they may result in pixel output values that are different from the input values[1] with possible chromaticity shifts [8]. It is, therefore, desirable to employ vector approaches in color image processing. However, few such attempts have been reported in the literature. Vector median filters (VMF) [9], [10] and their variates [11], [12] represent the only vector approaches proposed for color image processing. Vector approaches have also been used in other tasks, including restoration [13], [14], and edge detection [15], [16].

VMF are derived as MLE estimates from exponential distributions. If we consider, however, directional data, MLE estimates are not very appropriate [17]. This can be interpreted in our case as the fact that the VMF may not preserve the color chromaticity, with analogous visual results. VDF, on the other hand, perform optimally in this sense. Still, VDF do not take into account the image brightness when processing the image vectors. To compensate for that, VDF can be made to operate in cascade with grey-scale image processing filters, i.e., filters that operate on the brightness component. VDF find applications in color image processing and in areas that involve multispectral images, i.e., satellite imaging and multispectral biomedical image processing; moreover, VDF have been used in color image segmentation [18] by employing a clustering approach; the present study is confined to applications in color image restoration assuming various noise models.

The rest of the paper is organized as follows. In Section II, we review briefly the definition of VDF, and then, we study them in the framework of spherical (directional) estimators. The statistical and deterministic properties of VDF are analyzed in Section III. In Section IV, we present implementation details, and Section V introduces the extension of VDF to double-window structures. Section VI contains an extensive evaluation of their performance along with comparative results. In order to incorporate perceptual criteria in the comparisons, the error is measured in the $L^*a^*b^*$ space, which is known as a space where equal color differences result in equal distances [19]. Moreover, an indication of the chromaticity error is obtained by measuring the error on the Maxwell triangle. Finally, we draw our conclusions and give suggestions for further work in Section VII.

[1] Independent processing of the R, G, and B channels may rearrange the vectors' components and result in extraneous chromaticities in the output image.

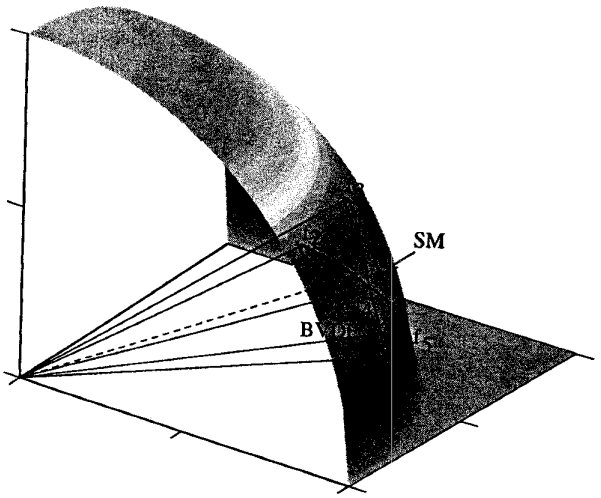

Fig. 1. SM and BVDF for spherical data. The input set consists of the five vectors $\boldsymbol{f}_1, \cdots, \boldsymbol{f}_5$. The BVDF is always one of the input samples ($\boldsymbol{f}_4$); this is not the case for SM.

II. Directional Estimators

In this section, we review the definition of VDF introduced in [1], and we study their relation to statistical estimators of directional data.

A. Vector Directional Filters (VDF)

The notation used in [1] is employed here. A multichannel signal is represented as $\boldsymbol{f}(x)$: $Z^l \rightarrow Z^m$. A window $W \in Z^l$ of finite size n is implied in all operations if not stated otherwise, and the pixels in W are denoted as $x_i, i = 1, 2, \cdots, n$. $\boldsymbol{f}(x_i)$ is an m-D vector in the vector space defined by the m signal channels; for convenience, it will be denoted as $\boldsymbol{f}_i$. For the case of color image processing $l = 2$, and $m = 3$. However, any value of $m \geq 2$ can be assumed in most of the results presented, implying *m-channel image processing*. The definition of VDF follows:

Definition 1: Let the input set $\{\boldsymbol{f}_i, i = 1, 2, \cdots, n\}$, and let α_i correspond to $\boldsymbol{f}_i$ and be defined as

$$\alpha_i = \sum_{j=1}^{n} \mathcal{A}(\boldsymbol{f}_i, \boldsymbol{f}_j), \qquad i = 1, 2, \cdots, n \tag{1}$$

where $\mathcal{A}(\boldsymbol{f}_i, \boldsymbol{f}_j)$ denotes the angle between vectors $\boldsymbol{f}_i$ and $\boldsymbol{f}_j$. In the general case, $0 \leq \mathcal{A}(\boldsymbol{f}_i, \boldsymbol{f}_j) \leq \pi$, whereas for the case of color images, $0 \leq \mathcal{A}(\boldsymbol{f}_i, \boldsymbol{f}_j) \leq \pi/2$. An ordering of the α_i's

$$\alpha_{(1)} \leq \alpha_{(2)} \leq \cdots \leq \alpha_{(r)} \leq \cdots \leq \alpha_{(n)} \tag{2}$$

implies the same ordering to the corresponding $\boldsymbol{f}_i$'s

$$\boldsymbol{f}^{(1)} \leq \boldsymbol{f}^{(2)} \leq \cdots \leq \boldsymbol{f}^{(r)} \leq \cdots \leq \boldsymbol{f}^{(n)}. \tag{3}$$

The first term in (3) constitutes the output of the *basic vector directional filter* (BVDF), whereas the first r terms of (3) constitute the output of the *generalized vector directional filter* (GVDF):

$$\boldsymbol{f}^{(1)} = \text{BVDF}[\boldsymbol{f}_1, \boldsymbol{f}_2, \cdots, \boldsymbol{f}_n] \tag{4}$$

$$\{\boldsymbol{f}^{(1)}, \boldsymbol{f}^{(2)}, \cdots, \boldsymbol{f}^{(r)}\} = \text{GVDF}[\boldsymbol{f}_1, \boldsymbol{f}_2, \cdots, \boldsymbol{f}_n], \quad 1 \leq r \leq n. \tag{5}$$

■

As can be verified from the above definition, the BVDF outputs the input vector that minimizes the sum of angles with all the other vectors within the processing window; the GVDF generalizes it since it outputs the set of vectors for which the above sum is *small*. The GVDF output should subsequently be passed through a second filter in order to produce a single output vector. This step may only consider the magnitudes of the vectors $\boldsymbol{f}^{(i)}, i = 1, 2, \cdots, r$, since after GVDF processing, these vectors have (approximately) the same direction in the vector space [1]. As a result, GVDF separate the processing of color vectors into directional processing and magnitude processing. This issue is deferred until Section IV, where we discuss the implementation of VDF.

B. Spherical Median

1) Population Spherical Median: The median of a distribution on the real line and the spatial median are each defined as that point from which the expected distance to a random value of the given distribution is minimized [20]. For a spherical (directional) distribution (Θ, Φ)[2] [21], distance D on the surface of the sphere is defined as the minimum arc length between two points. This leads to the notion of the spherical median (SM) direction [4].

Definition 2: $(\tilde{\theta}, \tilde{\phi})$ is the SM direction of the distribution of (Θ, Φ) if it minimizes

$$E\{D[(\Theta, \Phi), (\theta, \phi)]\} \equiv E(\Theta^*), \quad (\Theta^* = \cos^{-1}[\Lambda\lambda + M\mu + N\nu]) \tag{6}$$

over all choices (θ, ϕ), where (Λ, M, N) and (λ, μ, ν) are the direction cosines of (Θ, Φ) and (θ, ϕ), respectively. Thus, (6) minimizes the expected angular difference between the two unit vectors; by way of comparison, the mean direction minimizes $E[1 - \cos\Theta^*]$. ■

[2]Spherical data are usually represented with the polar coordinates Θ (colatitude) and Φ (latitude).

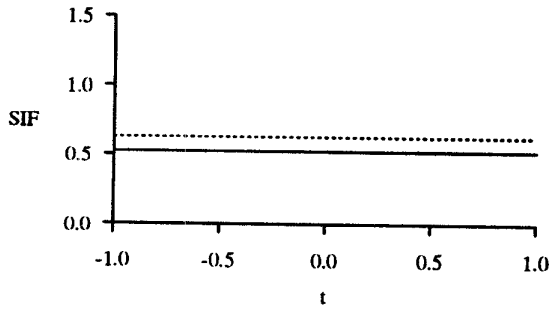

Fig. 2 Standardized influence function for the spherical median for two values of k; $k = 1$ (dotted curve) and $k = 10$ (solid curve).

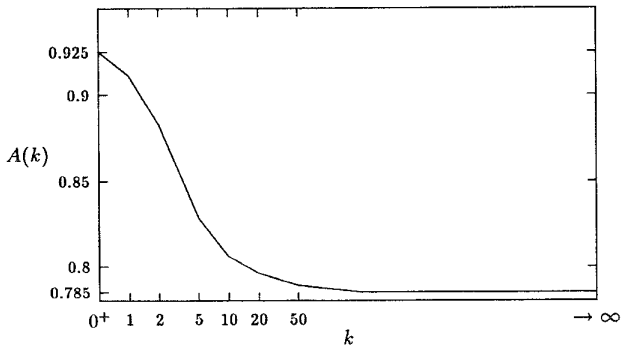

Fig. 3. Asymptotic relative efficiency of SM versus the mean direction for different values of k (see text for explanation).

2) Sample Spherical Median: Let $(\theta_1, \phi_1), \cdots, (\theta_n, \phi_n)$ be a random sample from a spherical distribution, and write $(\lambda_i, \mu_i, \nu_i) = (\sin\theta_i \cos\phi_i, \sin\theta_i \sin\phi_i, \cos\theta_i)$ for the direction cosines of the ith observation, $1 \leq i \leq n$.

Definition 3 [4]: The sample SM (SSM) is defined as the point from which the sum of the arc lengths to the data points is minimized. For a given point (λ, μ, ν), this sum is given as

$$D(\lambda, \mu, \nu) = \sum_{i=1}^{n} \cos^{-1}(\lambda_i \lambda + \mu_i \mu + \nu_i \nu). \qquad (7)$$

■

From the above definitions, it is obvious that the direction of the BVDF output is the SSM with the added constraint for the filter output to be one of the input vectors; this constraint is justified in order to avoid iterative algorithms for finding the solution. The above observation draws an analogy between VDF and VMF. The former results from the spherical median and is constrained to one of the input vectors, whereas the latter results from the spatial median with the same constraint. From a slightly different point of view, VDF and VMF both result from vector ordering using the aggregate ordering principle [22], the difference being the ordering criterion. VDF use the angles between the image vectors, whereas VMF employ the distances between the image vectors.

For the case at hand, i.e., color image processing, it is very important that the chrominance of the color vectors is preserved [19], which in turn implies that the vectors' direction should be preserved. The SM results in the least error estimation of the angle location. Consequently, the BVDF seems to be an appropriate directional filter for the case of color images. The operation of SM and BVDF for spherical data is illustrated in Fig 1, where the minimization property of these operators is shown. It should be noted at this point that in practice, color image data are not pure spherical data since the magnitudes of the image vectors vary at different pixels. However, VDF disregard the vectors' magnitudes and treat them purely as directional data.

III. Properties

In this section, statistical and deterministic properties of VDF are studied. We confine ourselves mainly to the BVDF in this section due to its amenability for mathematical treatment.

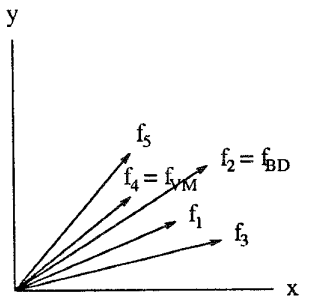

Fig. 4. Set of 2-D vectors. BVDF output (f_{BD}) is always the middle vector (f_2). This is not necessarily the case for the VMF output ($f_{VM} = f_4$).

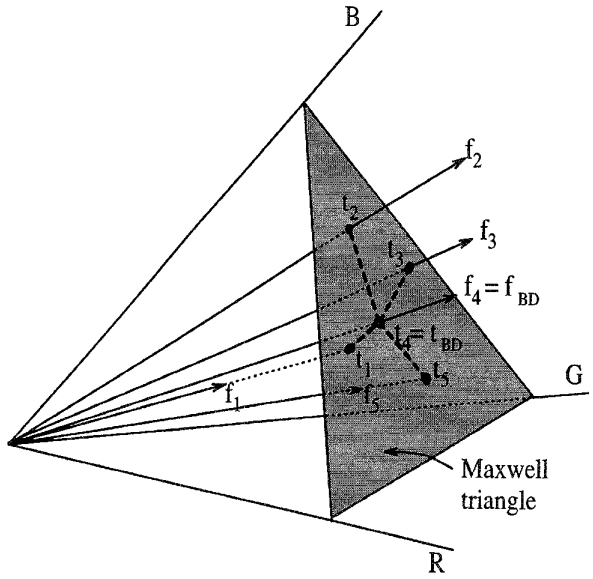

Fig. 5. Minimization property on the Maxwell triangle (see text for explanation).

However, some of the properties are also valid in the case of GVDF.[3]

A. Statistical Properties

The relation that has been established between SM and BVDF enables the study of the latter's statistical properties since they parallel closely the properties of SM for which adequate results are available in the statistical literature. In this section, we briefly summarize these properties in order to characterize BVDF in the framework of statistical estimators.

The robustness measures that characterize an estimator are the *breakdown point* and the *influence function* [23]. The breakdown point is the smallest fraction of outlier contamination that can cause an estimator to become unreliable. For spherical data, it is known that the SM attains a 50% breakdown point [3]. Therefore, the direction estimation of the BVDF possesses the same breakdown point, like the scalar median [24].

[3] A property trivial to establish for both BVDF and GVDF is their nonlinearity.

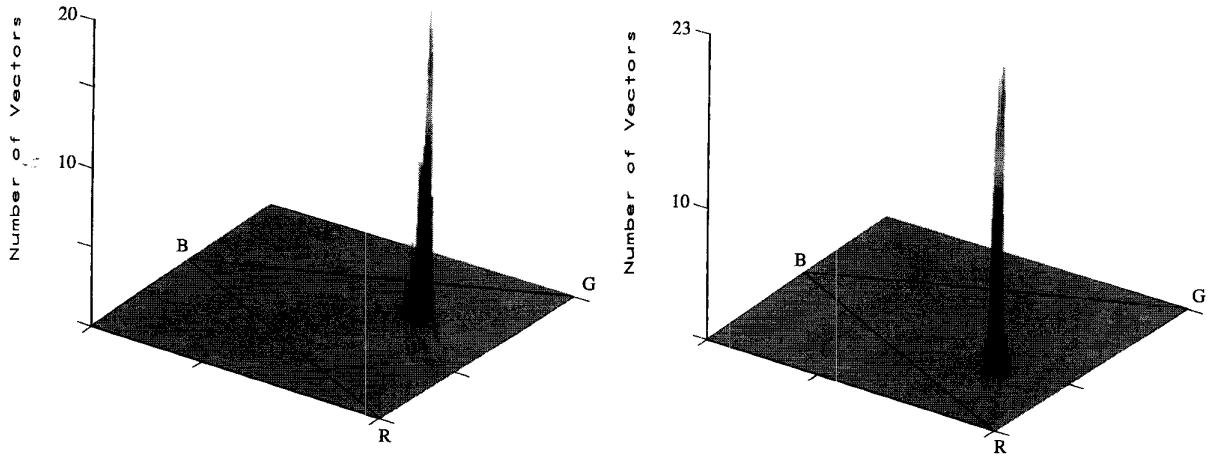

Fig. 6. Perspective plots of the number of image vectors intersecting the Maxwell triangle at the same point.

The influence function $IF(x;T,F)$ of an estimator T indicates the effect of a single outlier on the performance of the estimator at a point x. The supremum of IF over x, which is called the *gross-error sensitivity* (GES) γ, measures the worst effect of a contamination at any point x. If GES is finite, then the estimator is said to be bias-robust (B-robust). However, GES is often bounded if the parameter space is bounded, which is the case for spherical data. In that case, the concept of B-robustness needs to be modified [17]. This has led to the introduction of standardized B-robustness (SB-robustness), which is defined in terms of the standardized GES (SGES) γ^*. SGES measures the maximum bias relative to a measure of dispersion of the underlying distribution and is more appropriate for spherical data than GES [17]:

$$\gamma^* = \sup_{\mathcal{F}} \gamma(T,F)/S(F) = \sup_{\mathcal{F}} \sup_{x} SIF(x;T,F,S) \tag{8}$$

where SIF is the standardized IF with respect to $S(F)$. Assuming a von Misses–Fisher distribution[4] on the q-D sphere, SIF can be numerically calculated for the SM [3]. This is shown in Fig 2 for two k values (k is the concentration parameter of the von Misses-Fisher distribution). Fig 2 demonstrates that SIF is constant, depending only on k [3]. Consequently, the SM and the BVDF estimation of the direction is SB-robust. Moreover, it has constant norm of influence like the usual median.

The asymptotic relative efficiency (ARE) of SM compared with the mean direction, for the above mentioned distribution, is a function $A(k)$ of the parameter k, given as [4]

$$A(k) = \frac{k\pi^2 I_1^2(k)}{8\sinh^2(k)(\coth k - 1/k)}. \tag{9}$$

Numerical calculations indicate that $A(k)$ decreases monotonically from its value as $k \to 0^+ (A(0^+) = 0.925)$ to its value as $k \to \infty (A(\infty) = 0.785)$. A plot of $A(k)$ is shown in Fig 3. From a practical point of view, the higher efficiencies for more disperse distributions suggest that SM may be rather more useful, as an alternative to the mean, than its counterparts in the plane and on the line [4].

[4]The von Misses–Fisher distribution is the most commonly used distribution in directional data analysis [3]. It is defined parametrically, according to a concentration parameter k. For $k = 0$, it reduces to the uniform distribution on the sphere. Large values of k indicate a high degree of concentration of the data.

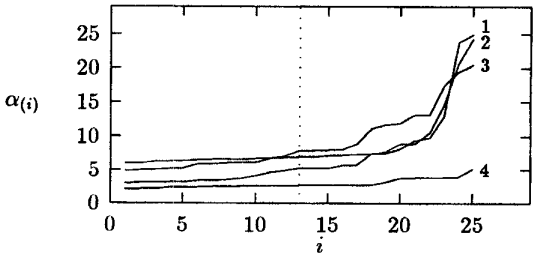

Fig. 7. $\alpha_{(i)}$ versus i (see text for explanation).

B. Deterministic Properties

In this section, basic deterministic properties of VDF that make them appropriate in multichannel image processing are presented. It is verified that VDF behave analogously to the scalar median since they are characterized by similar properties. The first three properties have been proved elsewhere [25], and we briefly summarize them here for the completeness of the paper.

1) Preservation of Step Edges: Let a vector-valued signal

$$\boldsymbol{f}(i) = \begin{cases} \boldsymbol{f}_1, & \text{if } i < i_0 \\ \boldsymbol{f}_2, & \text{if } i \geq i_0 \end{cases} \tag{10}$$

where $\boldsymbol{f}_1 \neq \boldsymbol{f}_2$. This is a step edge for vector-valued signals. It is trivial to establish that this signal is a root of the BVDF, regardless of the window size. This signal is also a root of the GVDF if $r \leq \lfloor n/2 \rfloor + 1$ (see (5)), where $\lfloor \cdot \rfloor$ denotes integer part.

2) Invariance Under Scaling and Rotation: Scaling by a scalar value and rotation of the coordinate system do not affect the angle between two vectors, and therefore, BVDF are invariant under these operations:

$$\text{BVDF}[\beta\boldsymbol{f}_1, \beta\boldsymbol{f}_2, \cdots, \beta\boldsymbol{f}_L] = \beta \cdot \text{BVDF}[\boldsymbol{f}_1, \boldsymbol{f}_2, \cdots, \boldsymbol{f}_L] \tag{11}$$

$$\text{BVDF}[\mathcal{R}\{\boldsymbol{f}_1, \boldsymbol{f}_2, \cdots, \boldsymbol{f}_L\}] = \mathcal{R}\{\text{BVDF}[\boldsymbol{f}_1, \boldsymbol{f}_2, \cdots, \boldsymbol{f}_L] \tag{12}$$

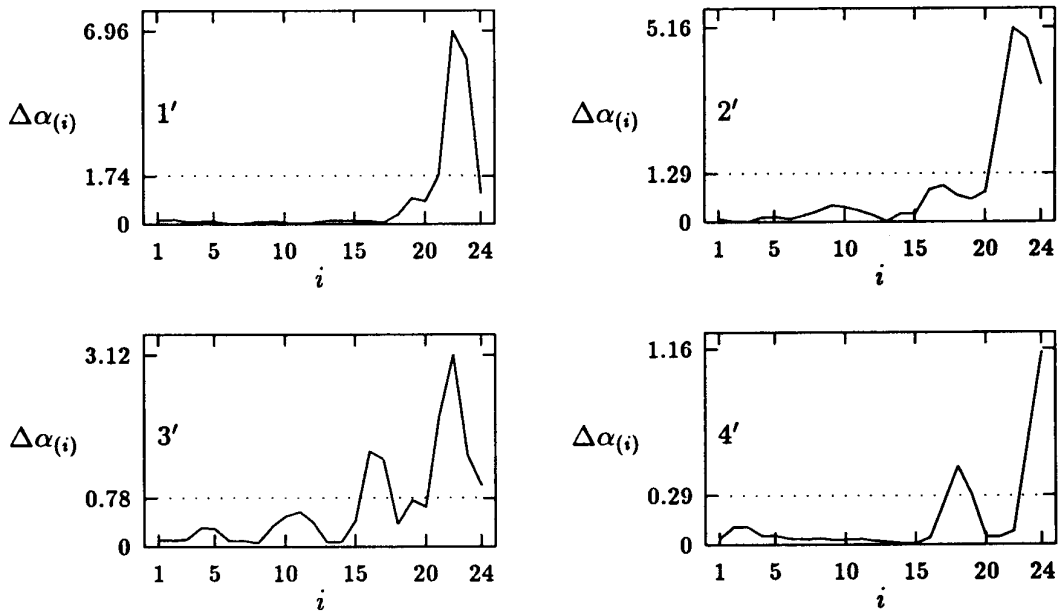

Fig. 8. Derivatives of the curves $\alpha_{(i)}$ shown in Fig 7.

where β is scalar, and $\mathcal{R}\{\cdot\}$ denotes the rotation operation. However, the BVDF is not invariant to bias since the addition of a (constant) vector changes the angles between vectors:

$$\begin{aligned}\text{BVDF}[\boldsymbol{f}_1 + \boldsymbol{c}, \boldsymbol{f}_2 + \boldsymbol{c}, \cdots, \boldsymbol{f}_L + \boldsymbol{c}] \\ \neq \text{BVDF}[\boldsymbol{f}_1, \boldsymbol{f}_2, \cdots, \boldsymbol{f}_L] + \boldsymbol{c}.\end{aligned} \tag{13}$$

Similarly, the GVDF is also invariant under scaling and rotation but not invariant to bias.

3) Existence of and Convergence to Root Signals: As already proved in property A, a step edge is a root signal of the BVDF, which proves the existence of root signals. Furthermore, repeated application of the BVDF will eventually produce a signal that is a root signal. This property is very similar to vector median filters. A proof and further details on the roots of BVDF can be found in [25].

If we confine ourselves in 2-D vectors (2-channel signals), then it is possible to characterize the root signals of the BVDF with a simple condition. A signal $\boldsymbol{f}_{(i)}$ is a root of the BVDF of length $N = 2m + 1$ iff, for all n, $\boldsymbol{f}_{(n)}$ satisfies

$$\frac{\boldsymbol{f}_{(l)_2}}{\boldsymbol{f}_{(l)_1}} \geq \frac{\boldsymbol{f}_{(n)_2}}{\boldsymbol{f}_{(n)_1}} \geq \frac{\boldsymbol{f}_{(j)_2}}{\boldsymbol{f}_{(j)_1}}, \qquad n - m \leq l < n < j \leq n + m \tag{14}$$

where $\boldsymbol{f}_{(i)_x}$ denotes the xth component (channel) of sample $\boldsymbol{f}_{(i)}$. This condition stems from the fact that in two dimensions, the BVDF is always the vector that lies in the middle of all the vectors (the exact equivalent of the scalar median).[5] Equation (14) simply expresses in mathematical terms this property, making use of the tangents of the vector angles (see Fig 4).

[5] Note that this is not always the case for the vector median filter; see Fig. 4, for example, where $\boldsymbol{f}_2$ is the BVDF output, whereas the output of the VMF is $\boldsymbol{f}_4$.

4) Minimization Property on the Maxwell Triangle: Let $\boldsymbol{t}_i, i = 1, 2, \cdots, L$ be the points of intersection between the vectors $\boldsymbol{f}_i, i = 1, 2, \cdots, L$ and the Maxwell triangle, and let $\text{BVDF}[\boldsymbol{f}_1, \boldsymbol{f}_2, \cdots, \boldsymbol{f}_L] = \boldsymbol{f}_{BD}$. Then, if we assume that the points $\boldsymbol{t}_i$ are concentrated in a small area on the Maxwell triangle, the point $\boldsymbol{t}_{BD}$ is the *spatial median* [20] of the points $\boldsymbol{t}_i$.

Proof: Let $\boldsymbol{f}_i^t, i = 1, 2, \cdots, L$ denote the vectors being formed by connecting the origin with the points $\boldsymbol{t}_i, i = 1, 2, \cdots, L$. By assumption, the points $\boldsymbol{t}_i$ are concentrated on the Maxwell triangle, and therefore, the vectors $\boldsymbol{f}_i^t, i = 1, 2, \cdots, L$ are approximately of equal length. In that case, the VMF of $\boldsymbol{f}_i^t$ is the $\boldsymbol{f}_{BD}^t$ [1]:

$$\begin{aligned}\text{VMF}[\boldsymbol{f}_1^t, \boldsymbol{f}_2^t, \cdots, \boldsymbol{f}_L^t] &= \text{BVDF}[\boldsymbol{f}_1^t, \boldsymbol{f}_2^t, \cdots, \boldsymbol{f}_L^t] \\ &= \boldsymbol{f}_{BD}^t.\end{aligned} \tag{15}$$

Consequently, $\boldsymbol{f}_{BD}^t$ minimizes the sum of the Euclidean distances between the vectors $\boldsymbol{f}_i^t$:

$$\begin{aligned}&\sum_{i=1}^{L} \|\boldsymbol{f}_{BD}^t - \boldsymbol{f}_i^t\| \leq \sum_{i=1}^{L} \|\boldsymbol{f}_j^t - \boldsymbol{f}_i^t\|, \quad \forall j \Rightarrow \\ &\sum_{i=1}^{L} \|\boldsymbol{t}_{BD} - \boldsymbol{t}_i\| \leq \sum_{i=1}^{L} \|\boldsymbol{t}_j - \boldsymbol{t}_i\|, \quad \forall j.\end{aligned} \tag{16}$$

Q.E.D.

A graphical illustration of the above property is shown in Fig. 5. This property demonstrates in mathematical terms the fact that VDF preserve the chromaticity of the image colors, a measure of which is taken from the intersection points. In other words, VDF select the output vector that results in the least distance error estimate on the Maxwell triangle.

It should be noted that the assumption made concerning the concentration of the points $\boldsymbol{t}_i$ is (in most cases) not a strong one since, at least in image areas with no strong

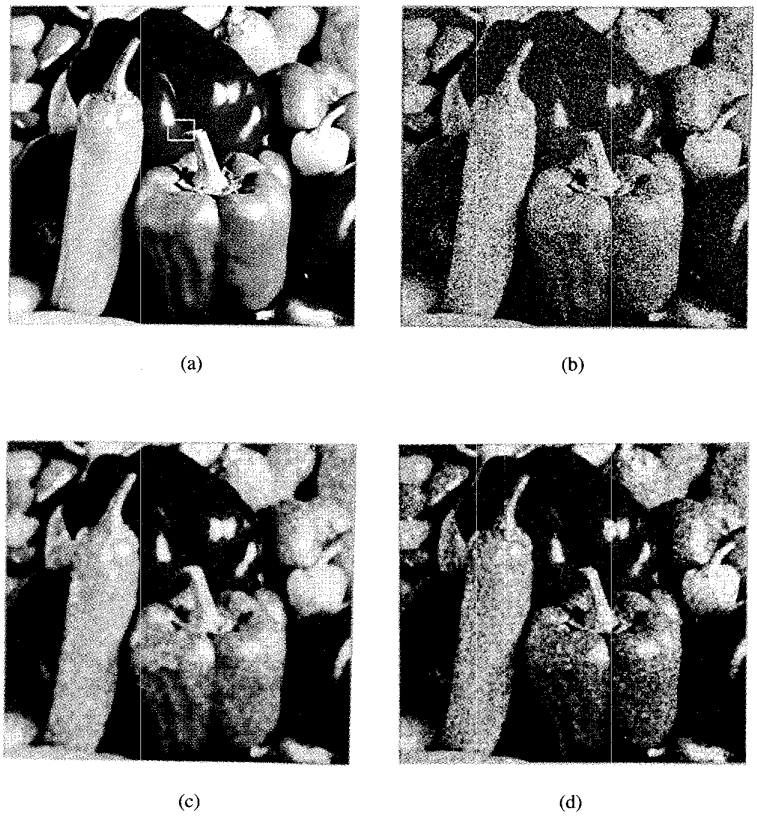

(a) (b)

(c) (d)

Fig. 9. (a) Color image "peppers"; (b) image "peppers" corrupted by a mixture of Gaussian ($\sigma = 60$) and 6% impulsive noise; (c) GVDF_DW_αTM results; (d) VMF results.

edges, the image vectors tend to be locally clustered in the directional sense. This can be observed in Fig. 6, where the perspective plots of the number of image vectors intersecting the Maxwell triangle at the same point have been drawn for two 20×20 neighborhoods (with no strong edges) taken from two images. In the opposite case (strong edges present), we cannot rigorously prove this assertion since the vectors $\boldsymbol{f}_i^t, i = 1, 2, \cdots, L$ are not of equal length. However, using computer simulations, we have demonstrated the validity of this property for numerous example cases that were tested. An intuitive justification of that relies on the fact that the BVDF chooses the vector $\boldsymbol{f}_{BD}$ *most centrally located* (in the directional sense) in the input population $\boldsymbol{f}_i$; therefore, the point $\boldsymbol{t}_{BD}$ will *always* be centrally located in the population $\boldsymbol{t}_i$.

IV. Implementation of VDF

The implementation of VDF can be studied along different axes, regarding the various issues that are involved in that. At first, we need to devise techniques for accelerating the computations since they involve time-consuming operations (square roots, inverse cosines, etc.). This can be easily achieved based on the observation that as the processing window (of size n) moves within the image, then after each move, only m ($m < n$, and usually, $m = \sqrt{n}$) new pixels are considered whose angles with the other vectors have to be computed. The angles of the rest of the $n - m$ vectors are simply updated. This implementation has led to considerable computational savings, especially in the case of relatively large windows (for a 7×7 window, the computational savings come to 81.5%).

Next, GVDF involve a parameter r (see (5)) that needs to be specified for a particular implementation. Basically, there are two ways of choosing r: adaptive and nonadaptive. The case of adaptive selection of r is desirable since it may produce a better output vector set. When there is a high variation of the color in the image (edges), the $\alpha_{(i)}$ sequence will present a large discontinuity that separates the vectors in the two regions. In this case, only vectors from one region will be output by an adaptive GVDF. At a uniform region, on the other hand, the $\alpha_{(i)}$ sequence is growing quite regular, and a lot of vectors are taken that may result in improved noise rejection. These issues are illustrated in Fig 7, where the ordered sequence $\alpha_{(i)}$ has been plotted for four different placements of the window W (5×5) on the "mandrill" image (Fig. 11). Three out of the four window positions correspond to rapidly changing areas (hair texture, eyes-lash border, beard), whereas, the fourth one corresponds to a smooth area (nose). The first three window placements give rise to curves 1, 2, and 3, respectively, whereas the fourth gives rise to curve 4. As can be observed, for large i values, $\alpha_{(i)}$ grows very rapidly in the case of nonsmooth image areas. However, in all cases, $\alpha_{(i)}$ is small and almost constant for smaller i values. Therefore,

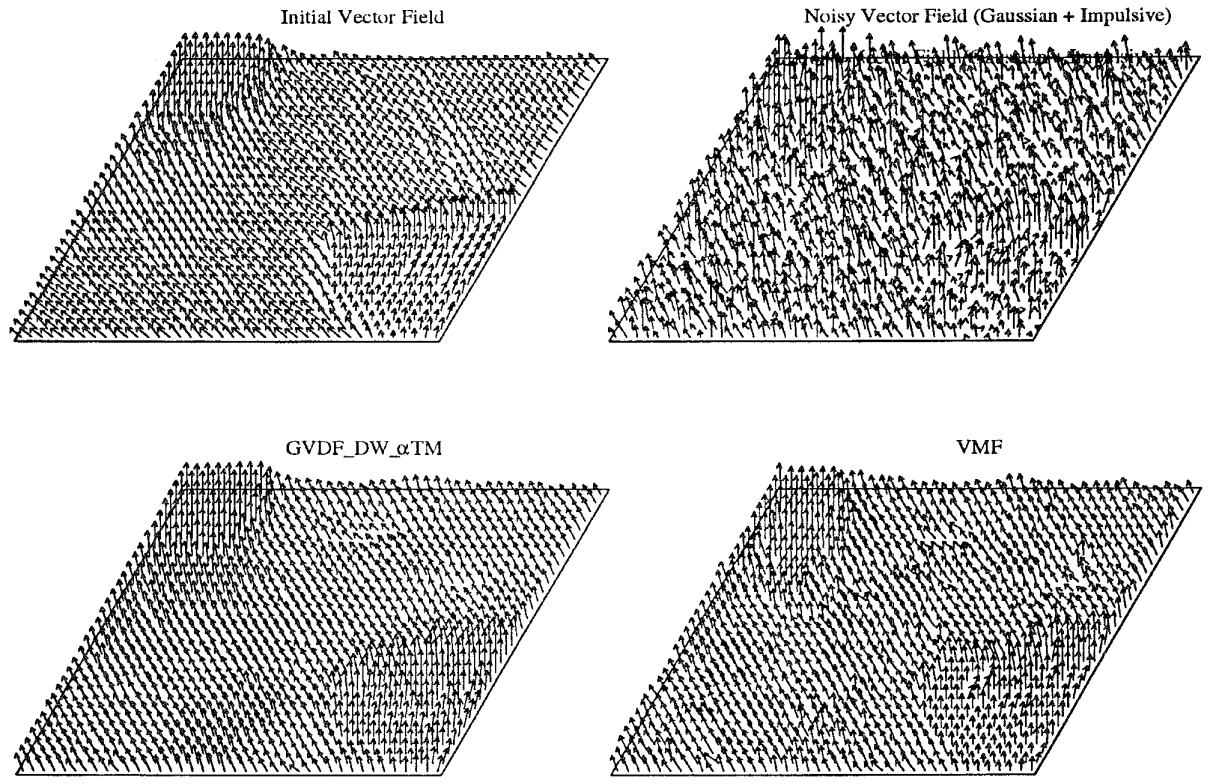

Fig. 10. Vector field for the window shown on Fig 9: (top left) Initial; (top right) noisy; (bottom left) GVDF_DW_αTM; (bottom right) VMF.

we suggest a value of $r = \lfloor n/2 \rfloor + 1$, for a window of size n for a nonadaptive selection of r. As can be verified from Fig. 7, this represents a "safe value" since $\alpha_{(i)}$ starts increasing for i values much larger than $\lfloor n/2 \rfloor + 1$. To implement the adaptive selection of r, we take the derivative of the sequence $\alpha_{(i)}$ and cut it at the first discontinuity that exceeds $\tau\%$ of the maximum derivative. This is illustrated in Fig. 8 for the four angle sequences shown in Fig. 7 and for $\tau = 25$. This value of τ has been set through experimentation; more importantly, these experiments have verified that this value is not crucial for the filter performance. In our implementations of GVDF, we have adopted the adaptive version since our simulations have shown that it performs slightly better than the nonadaptive version.

Finally, GVDF need to be combined with appropriate (magnitude processing) filters in order to produce a single output vector at each pixel. In the case of BVDF, no such filter is present; this represents a drawback since the magnitude information carried by the vectors is not taken into account when computing the output vector. GVDF can alleviate that by operating in cascade with filters that consider the magnitude information. The application of GVDF results in a set of vectors with (approximately) the same direction in the color space [1]. More specifically, GVDF eliminate from the input vectors the ones with *atypical* directions and output the ones centrally located in the population. Consequently, GVDF achieve, in a sense, production of a (locally) *single-channel* signal since the set of vectors produced contains samples in (almost) the same direction.

The GVDF output should subsequently be passed through a filter $\mathcal{F}$ in order to produce a single output at each pixel. Since the GVDF output consists of vectors with (approximately) the same direction, $\mathcal{F}$ may consider only the magnitudes of the vectors, i.e., it can be *any grey-scale* image processing filter [26], [27]; depending on the application, smoothing filters (e.g., α-trimmed mean—αTM) or detail preserving filters (e.g., multistage max/median—MM [28]) can be employed. Referring to the definition of GVDF (see (5)), the above operation can be written as

$$\boldsymbol{f}_O = \mathcal{F}\{\boldsymbol{f}^{(1)}, \boldsymbol{f}^{(2)}, \cdots, \boldsymbol{f}^{(r)}\} \tag{17a}$$

$$= \mathcal{F}\{\text{GVDF}[\boldsymbol{f}_1, \boldsymbol{f}_2, \cdots, \boldsymbol{f}_n]\}. \tag{17b}$$

The above-described structure draws an analogy between GVDF and the *modified mean trimmed* (MTM) filters [29]. These filters operate by excluding the samples in the filter window that differ considerably from the median value and, subsequently, taking the mean of the remaining samples. It is well known that MTM perform very accurately both in gray-scale and in multichannel image processing [24]. GVDF follow the same principle in the multichannel case but employ a different criterion. Instead of utilizing the *distances* between the samples, they employ the *angles* between the vectors; vectors that form large angles with the rest of the samples are characterized as *directional outliers* and are excluded from further processing. The amount of trimming depends on the filter parameter r (in the adaptive case, the threshold τ). The smaller the r (or τ) is, the stronger the trimming. The two

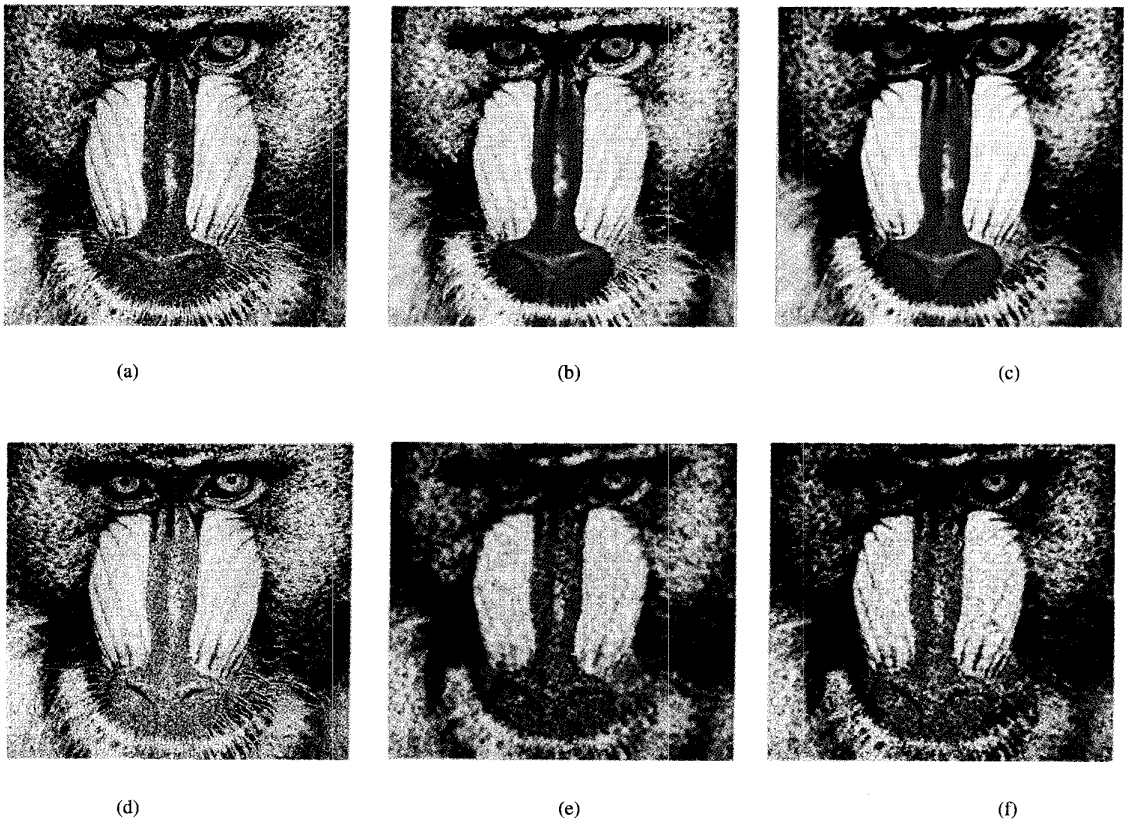

(a) (b) (c)

(d) (e) (f)

Fig. 11. Illustrative examples: (a) Image "mandrill" corrupted by 6% impulsive noise; (b) GVDF_DW_MM results; (c) VMF results; (d) image "mandrill" corrupted by Von Misses–Fisher noise ($k = 1$); (e) GVDF_αTM results; (f) VMF results.

extreme cases are $r = 1$ and $r = n$. In the former case ($r = 1$), the GVDF reduces to BVDF, and no magnitude processing is performed; in the later case ($r = n$), the GVDF output is the same as its input, and no directional processing is performed.

V. Double-Window Structures

Double-window (DW) filtering structures are known to perform very accurately in grey-level image processing [29], [24]. They do so by computing the median in a small window and then using pixel values from a larger window (the ones that satisfy a condition) to perform averaging. In other words, two distinguishable operations (computation of median and averaging) are performed using different windows. Each of these two windows plays a specific role; the small window is used for preserving the image details, whereas the large window is used in order to obtain a broad coverage of pixel values. Consequently, a more accurate approximation of the output value is achieved. This can also be extended to VDF processing. The two operations of directional processing and magnitude processing can be made to perform in two windows. This leads to the *double-window* GVDF (GVDF_DW).

Definition 4: Let W_1, W_2 be two windows with $W_1 \subset W_2$. Additionally, let $\boldsymbol{f}_{1_i}, i = 1, 2, \cdots, n$ be the image vectors in W_1, i.e., $\boldsymbol{f}_{1_i} \in W_1$ and $\boldsymbol{f}_{2_j}, j = 1, 2, \cdots, l$ be the image vectors in W_2 but not in W_1, i.e., $\boldsymbol{f}_{2_j} \in W_2 - W_1$. The application of GVDF to $\boldsymbol{f}_{1_i}, i = 1, 2, \cdots, n$ produces the output set $\{\boldsymbol{f}_1^{(1)}, \boldsymbol{f}_1^{(2)}, \cdots, \boldsymbol{f}_1^{(r)}\}$ (see Definition 1 and (5)) for the ordering of α_{1_i}'s $\alpha_1^{(1)} \leq \alpha_1^{(2)} \leq \cdots \leq \alpha_1^{(r)} \leq \cdots \leq \alpha_1^{(n)}$ (see (2)). The set $\{\boldsymbol{f}_1^{(1)}, \boldsymbol{f}_1^{(2)}, \cdots, \boldsymbol{f}_1^{(r)}\}$ is augmented with vectors from $W_2 - W_1$, and subsequently, it is used in (17) to compute the final output $\boldsymbol{f}_O$.

Let $\boldsymbol{f}_{2_j} \in W_2 - W_1$, and let α'_{2_j} correspond to $\boldsymbol{f}_{2_j}$ and be defined as

$$\alpha'_{2_j} = \sum_{i=1}^{n} \mathcal{A}(\boldsymbol{f}_{2_j}, \boldsymbol{f}_{1_i}). \tag{18}$$

Then, $\boldsymbol{f}_{2_j}$ is added to the set $\{\boldsymbol{f}_1^{(1)}, \boldsymbol{f}_1^{(2)}, \cdots, \boldsymbol{f}_1^{(r)}\}$ if the condition

$$\alpha'_{2_j} \leq \alpha_1^{(r)} \tag{19}$$

is satisfied. In other words, the outer window $W_2 - W_1$ contributes with the vectors $\boldsymbol{f}_{2_j}$ that diverge from the population $\boldsymbol{f}_{1_i}$ less than the divergence of the last considered vector ($\boldsymbol{f}_1^{(r)}$) from $\boldsymbol{f}_{1_i}$. ■

Definition 4 uses the inner window (W_1) to perform the directional ordering of the vectors; subsequently, vectors from the outer window ($W_2 - W_1$) are also used in the step of magnitude processing if they are *centrally located* within the population of vectors $\boldsymbol{f}_{1_i}, i = 1, 2, \cdots, n$. This is in analogy with the scalar DW filters that consider the pixels from the

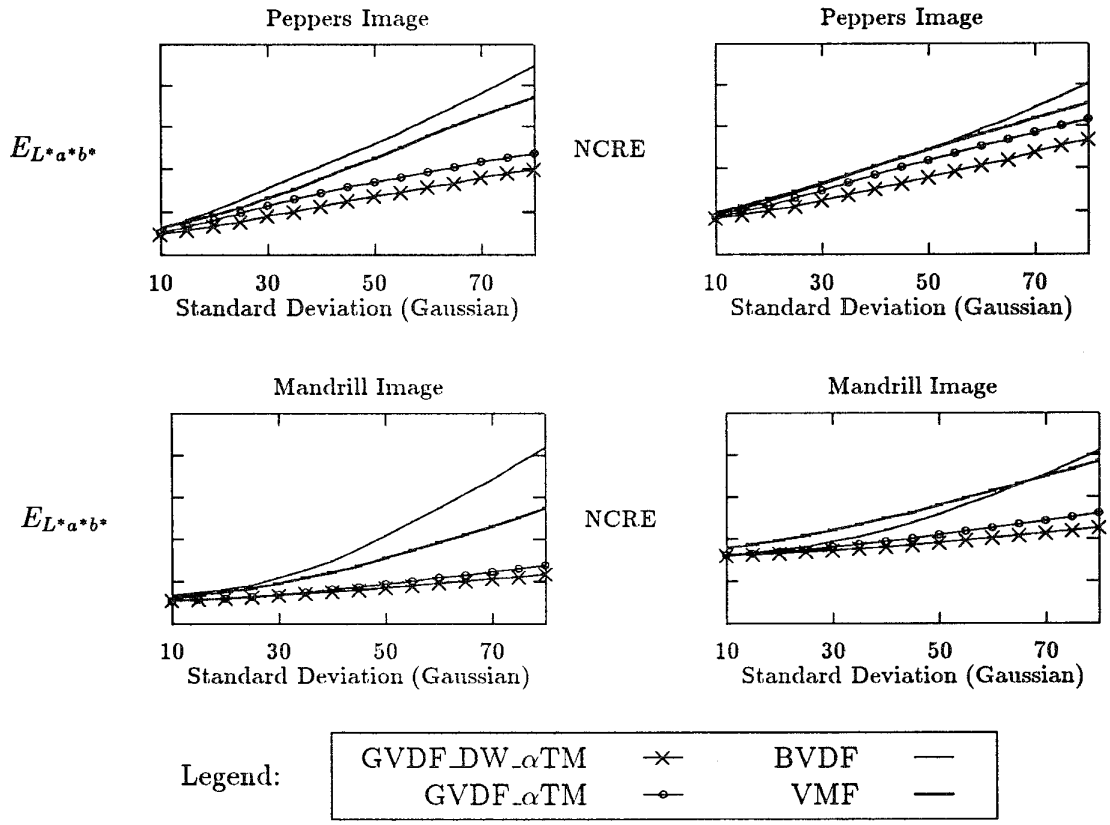

Fig. 12. Performance evaluation results for the case of Gaussian noise.

outer window if they are close to the median (centrally located on the line).

The rationale for the introduction of GVDF_DW is similar to the scalar case. The small (inner) window is used to compute accurate directional estimates, whereas the large (outer) window contributes to the magnitude processing step under the constraint of the (already) computed directional estimates. Consequently, more vectors are used to compute the filter output, resulting in a better estimate. Our computer experiments have demonstrated this, as will be shown in the following section.

VI. Experimental Results

We have conducted a set of experiments in order to evaluate VDF and compare their performance against the performance of VMF. The results of these experiments are presented in this section. Sample illustrative results are also presented to demonstrate the performance of the filters. In all cases, we have used 5×5 masks to implement the filters. A convention is used in the sequel for the naming of the filter structures. The magnitude processing filter abbreviation is appended to the directional processing filter abbreviation. Therefore, GVDF_DW_αTM stands for *double window* GVDF followed by an *α-trimmed mean*, and GVDF_MM stands for GVDF followed by a *multistage max/median filter*.

The images used in the experiments were RGB color images; the noise models implemented and tested were Gaussian, impulsive, Von Misses–Fisher, and Gaussian mixed with impulsive. For the noise models Gaussian, impulsive, and their mixture, a channel correlation factor of 0.5 has been used to simulate the channel correlation in color images. For the case of Von Misses–Fisher noise, the above does not apply since this distribution refers to spherical data and is computed after transforming the data to spherical coordinates. The value of 0.5 for the channel correlation has been chosen as an "unbiased" estimate of the true correlation.

A. Illustrative Examples

The performance of VDF has been subjectively estimated using real color images corrupted by artificial noise. We present here illustrative examples that demonstrate the usefulness of VDF in color image processing. The first result refers to the color image "peppers" shown in Fig. 9(a). Fig. 9(b) shows the same image corrupted by a mixture of Gaussian and impulsive noise. The Gaussian distribution is characterized by zero mean and standard deviation $\sigma = 60$, and 6% of the impulses have been added to the signal. Both the Gaussian and the impulsive noise have been modeled using a channel correlation factor $\rho = 0.5$. The results after processing Fig. 9(b) with GVDF_DW_αTM are presented in Fig. 9(c); Fig. 9(d) shows the same results for the case of VMF filtering for comparison purposes. As can be verified, GVDF perform very efficiently in the removal of noise. Moreover, they effectively combine the directional processing characteristics

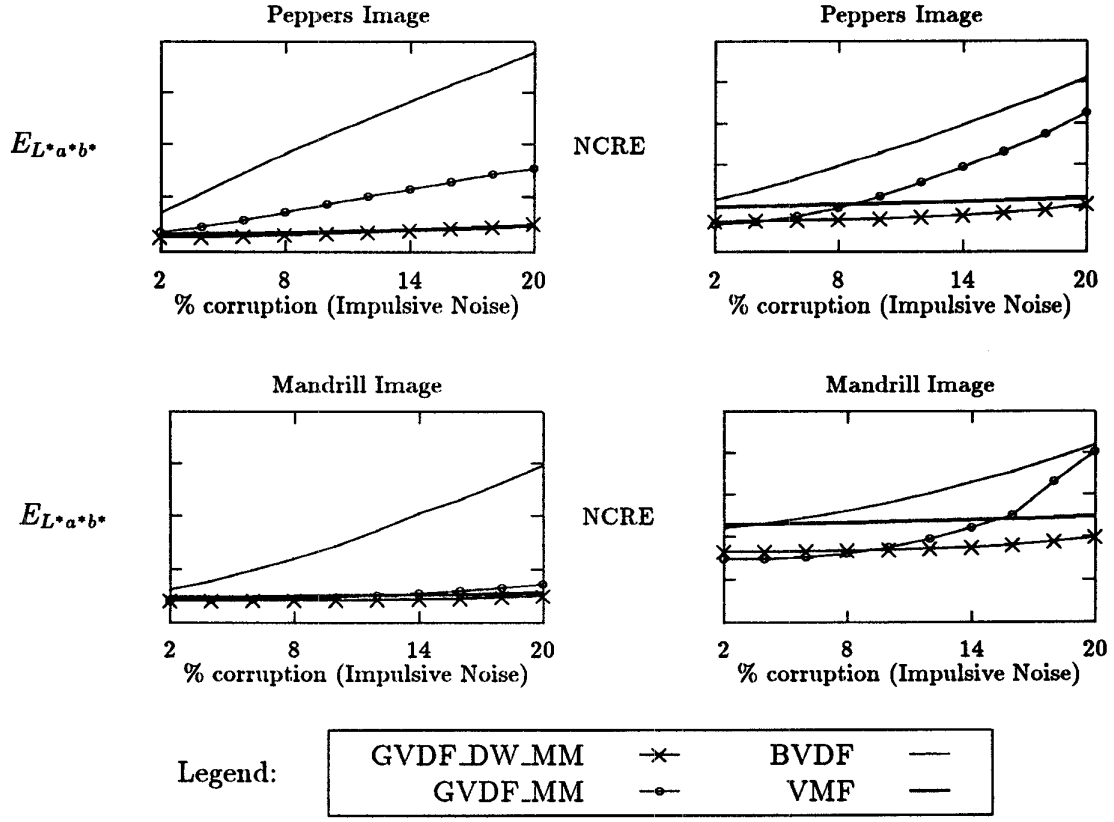

Fig. 13. Performance evaluation results for the case of impulsive noise.

(removal of vectors with atypical directions) with magnitude processing characteristics (efficiency of the α-trimmed mean filter in smoothing out Gaussian noise).

In order to impart a better appreciation as of the performance of the filters, we show in Fig. 10 the actual image vectors for the 40×32 window shown in Fig. 9 superimposed on the image data. The initial vector field is shown in Fig. 10(a), where one can easily distinguish the three different areas on the image: *red* part of pepper, *white* (reflectance) part of pepper, and *green* stem. In Fig. 10(b), the same window is presented, after it has been corrupted by noise, with obvious effect on the vector field. Fig. 10(c) and (d) show the restored vector field for the cases of GVDF_DW_αTM and VMF, respectively. As can be observed, the GVDF has almost completely restored the vector field with no noticeable deformations and clear boundaries between the three areas. On the contrary, the effects of noise still show up on the VMF result; a comparison of the two images (Fig. 10(c) and (d)) clearly favors the GVDF over VMF.

Illustrative examples for two other noise models are shown in Fig. 11 for the "mandrill" image. Fig. 11(a) shows the mandrill image corrupted with 6% impulsive noise, and Fig. 11(b) and (c) show the GVDF_DW_MM and VMF results, respectively. As can be verified, the results are comparable, but still, GVDF_DW_MM has a slightly better performance in preserving the fine details of the image (see the hair texture, for example). This can mainly be ascribed to the multistage max/median filter used as the magnitude processing filter, which is known to perform very accurately in preserving the fine image details.

In Fig. 11(d), a version of the mandrill image corrupted with Von Misses–Fisher noise ($k = 1$) is presented, and the filtering results are shown in Fig. 11(e) and (f). Fig. 11(e) is the GVDF_αTM, and Fig. 11(f) is the VMF result, respectively. Again, GVDF show superior performance and a more pleasing result for the human observer.

B. Performance Evaluation

In order to objectively evaluate the performance of VDF, we have used the two color images "peppers" (Fig. 9) and "mandrill" (Fig. 11) and the following evaluation procedure. For each image and for each of the noise models (described above), we have varied the corresponding parameter of the noise model[6] and measured two performance measures: $E_{L^*a^*b^*}$ and NCRE. $E_{L^*a^*b^*}$ refers to the mean absolute error measured in the $L^*a^*b^*$ space. It is known [19] that in this space, equal color differences result in equal distances, and therefore, $E_{L^*a^*b^*}$ is very close to the human perception of error in color images [30]. *Normalized chromaticity error* (NCRE) has

[6]For the case of mixed noise (Gaussian with impulsive), only the standard deviation of the Gaussian distribution was varied, and the percentage of impulses was constant and equal to 10%.

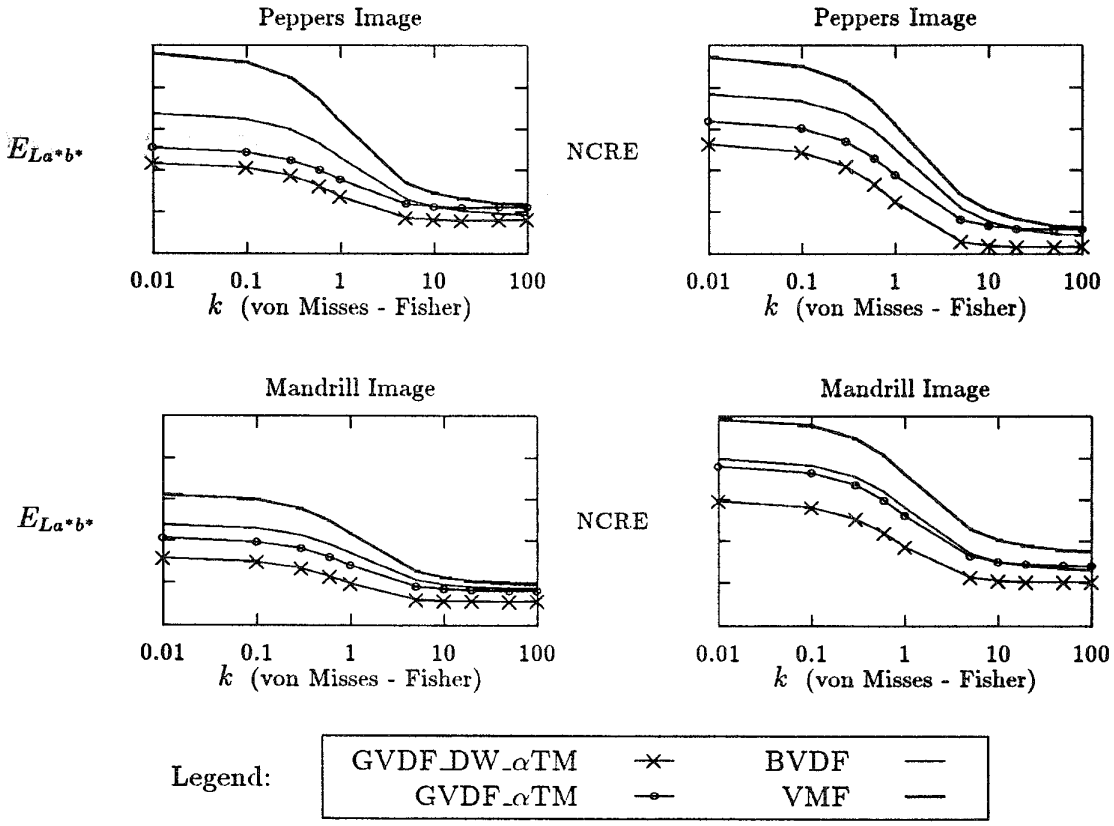

Fig. 14. Performance evaluation results for the case of Von Misses–Fisher noise.

been introduced in [1] and measures the distance of the color vectors on the Maxwell triangle. Since the color chromaticity is obtained from the intersection point on the Maxwell triangle, NCRE gives an indication of the chromaticity error. It has been adopted in this work since VDF are chromaticity preserving filters, and it is desirable to evaluate their performance with respect to that. It should be noted that NCRE should not be taken to be the *exact* chromaticity error since it is known that the Maxwell triangle is not a plane where equal color differences result in equal distances. Rather, NCRE gives an exact indication of the vectors' divergence from the original directions, which can be *qualitatively* interpreted as the chromaticity error.

The results obtained are shown in the form of plots in Figs 12–15 for the four noise models: Gaussian, impulsive, Von Misses–Fisher, and Gaussian mixed with impulsive, respectively. For the case of impulsive noise, the MM filter has been used as the magnitude processing filter. For the other noise models, MM has been replaced by the αTM filter. In all cases, we show the results of BVDF, GVDF followed by the corresponding magnitude processing filter, double window GVDF followed by the corresponding magnitude processing filter, and VMF.

As can be verified from the plots of Figs. 12–15, the performance of GVDF is at least equal and in most cases is superior to the performance of VMF. For the case of Gaussian noise (Fig. 12), GVDF_DW_αTM has by far the best performance with GVDF_αTM following next. The same remark is also valid for the case of Gaussian mixed with impulsive noise (Fig. 15). In the impulsive case (Fig. 13), where VMF is known to perform very accurately, GVDF_DW_MM is at least as accurate and in some cases slightly superior to the VMF. For the Von Misses–Fisher noise distribution, it is noted that larger k values indicate smaller noise levels, and consequently, we obtain decreasing curves (Fig. 14). GVDF_DW_αTM and GVDF_αTM perform more accurately, especially for small k values. For large k values, the noise tends to behave more like impulsive noise, and hence, VMF perform comparable to GVDF.

In conclusion, the results presented in Figs. 12–15 show the accuracy of directional processing in color images and, moreover, demonstrate the effectiveness of combining GVDF with efficient gray scale image processing filters. It should also be noted at this point that consistent results (with the ones presented above) have been obtained when using a variety of other color images and the same evaluation procedure. Figs. 12–15 presented here are simply representative of the performance of the filters evaluated.

VII. Conclusions

In this paper, we have studied VDF in the framework of directional estimators and have extensively evaluated their

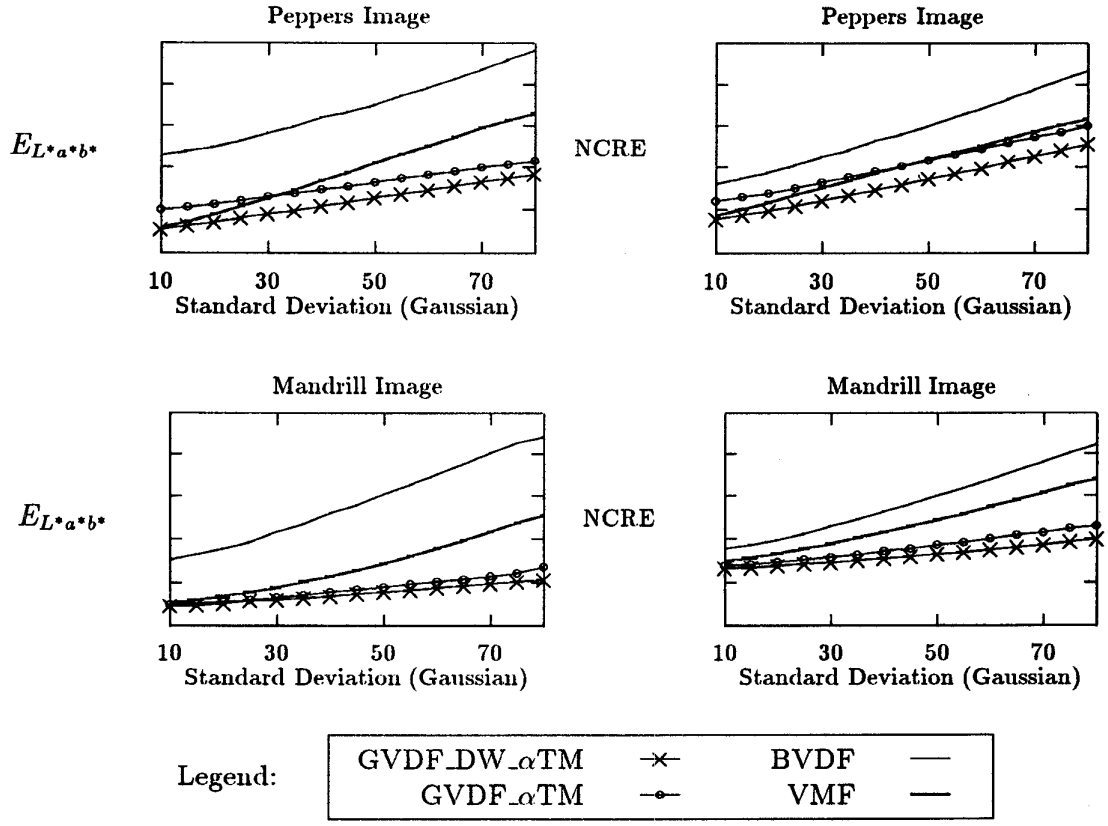

Fig. 15. Performance evaluation results for the case of Gaussian mixed with 10% impulsive noise.

performance. Their relation to the spherical median has been investigated, and their statistical and deterministic properties have been developed. Efficient computational schemes for their implementation have been employed, and their extension to double window structures has been proposed. Evaluation results have shown very accurate performance measures that compare very favorably to the VMF for various noise models. The advantage of VDF is the preservation of the chromaticity component, which is very important in visual perception. Moreover, GVDF can be combined with efficient grey-scale image processing filters, resulting in effective filtering structures.

Color image processing has receiving increased attention lately due to many important applications involved in color imaging. It has been recognized by many authors that processing of color image data as vector fields is desirable due to the correlation that exists between the image channels. Toward this end, VMF [9] and some variations [11], [12] have been introduced and studied recently. These filters are mainly based on distance ordering principles. VDF represent an approach where directional information is used to process the image vectors. Experimentation with this approach has shown very promising results. Future work in this area should address the processing of other multichannel images (e.g., satellite images and multispectral medical images) in the framework of VDF. Moreover, the issue of magnitude processing has not been fully investigated in the present work. More work is needed to establish the relation between directional and magnitude processing and, possibly, to derive more appropriate classes of magnitude processing filters to operate in cascade with GVDF.

REFERENCES

[1] P. E. Trahanias and A. N. Venetsanopoulos, "Vector directional filters—A new class of multichannel image processing filters," *IEEE Trans. Image Processing*, vol. 2, no. 4, pp. 528–534, Oct. 1993.

[2] R. Machuca and K. Phillips, "Applications of vector fields to image processing," *IEEE Trans. Pattern Anal. Machine Intell.*, vol. PAMI-5, no. 3, pp. 316–329, May 1983.

[3] D. Ko and T. Chang, "Robust M-estimators on spheres," *J. Multivariate Anal.*, vol. 45, pp. 104–136, 1993.

[4] N. I. Fisher, "Spherical medians," *J. Royal Stat. Society B*, vol. 47, no. 2, pp. 342–348, 1985.

[5] S. Naqvi, N. Galagher, and E. Coyle, "An application of median filtering to digital television," in *Proc. IEEE ICASSP*, Apr. 1986, pp. 2451–2454.

[6] R. Strickland, C. Kim, and W. McDonnel, "Digital color image enhancement based on the saturation component," *Opt. Eng.*, vol. 26, no. 7, pp. 609–616, July 1987.

[7] J. Bescos, I. Glaser, and A. Sawchuk, "Restoration of color images degraded by chromatic aberrations," *Appl. Opt.*, vol. 19, no. 22, pp. 3869–3876, Nov. 1980.

[8] J. Zheng, K. P. Valavanis, and J. M. Gauch, "Noise removal from color images," *J. Intell. Robot. Syst.*, vol. 7, no. 3, pp. 257–285, June 1993.

[9] J. Astola, P. Haavisto, and Y. Neuvo, "Vector median filters," *Proc. IEEE*, vol. 78, no. 4, pp. 678–689, Apr. 1990.

[10] M. Gabbouj, E. J. Coyle, and N. C. Gallagher, "An overview of median and stack filtering, " *Circuits, Syst., Signal Processing*, vol. 11, no. 1, pp. 7–45, 1992.

[11] S. Sanwalka and A. N. Venetsanopoulos, "Vector order statistics filtering of color images," in *Proc. 13th GRETSI Symp. Signal Image Processing*, 1991, pp. 785–788.

[12] R. C. Hardie and G. R. Arce, "Ranking in R^p and its use in multivariate image estimation," *IEEE Trans. Circuits Syst. Video Technol.*, vol. 1, no. 2, pp. 197–209, June 1991.
[13] N. P. Galatsanos, A. K. Katsaggelos, R. T. Chin, and A. D. Hillery, "Least squares restoration of multichannel images," *IEEE Trans. Acoust. Speech Signal Processing*, vol. 39, no. 10, pp. 2222–2236, Oct. 1991.
[14] N. P. Galatsanos and R. T. Chin, "Restoration of color images by multichannel Kalman filtering," *IEEE Trans. Acoust. Speech Signal Processing*, vol. 39, no. 10, pp. 2237–2252, Oct. 1991.
[15] P. E. Trahanias and A. N. Venetsanopoulos, "Color edge detection using vector order statistics," *IEEE Trans. Image Processing*, vol. 2, no. 2, pp. 259–264, Apr. 1993.
[16] A. Cumani, "Edge detection in multispectral images," *CVGIP: Graphical Models Image Processing*, vol. 53, no. 1, pp. 40–51, Jan. 1991.
[17] D. Ko and P. Guttorp, "Robustness of estimators for directional data," *Ann. Stat.*, vol. 16, no. 2, pp. 609–618, 1988.
[18] P. E. Trahanias, D. Karakos, and A. N. Venetsanopoulos, "Directional segmentation of color images," in I. Pitas, Ed., *1995 IEEE Workshop Nonlinear Signal Image Processing*, Neos Marmaras, Halkidiki, June 1995, pp. 515–518.
[19] W. K. Pratt, *Digital Image Processing*. New York: Wiley, 1991.
[20] B. M. Brown, "Statistical uses of the spatial median," *J. Royal Stat. Soc. B*, vol. 45, no. 1, pp. 25–30, 1983.
[21] K. V. Mardia, *Statistics of Directional Data*. London: Academic, 1972.
[22] V. Barnett, "The ordering of multivariate data," *J. Royal Stat. Soc. A*, vol. 139, part 3, pp. 318–343, 1976.
[23] F. Hampel, E. Ronchetti, P. Rousseevw, and W. Stahel, *Robust Statistics: An Approach Based on Influence Functions*. New York: Wiley, 1986.
[24] I. Pitas and A. N. Venetsanopoulos, "Order statistics in digital image processing." *Proc. IEEE*, vol. 80, no. 12, pp. 1893–1921, Dec. 1992.
[25] P. E. Trahanias and A. N. Venetsanopoulos, "Multichannel image processing using vector-angle ranking," in *Proc. SPIE Conf., Nonlinear Image Processing IV*, San Jose, CA, Jan. 30–Feb. 5, 1993.
[26] I. Pitas and A. N. Venetsanopoulos, *Nonlinear Digital Filters—Principles and Applications*. Norwell, MA: Kluwer, 1990.
[27] A. K. Jain. *Fundamentals of Digital Image Processing*. Englewood Cliffs, NJ: Prentice-Hall, 1989.
[28] G. R. Arce and R. E. Foster, "Detail-preserving ranked-order based filters for image processing," *IEEE Trans. Acoust. Speech Signal Processing*, vol. 37, no. 1, pp. 83–98, Jan. 1989.
[29] Y. H. Lee and S. A. Kassam, "Generalized median filtering and related nonlinear filtering techniques," *IEEE Trans. Acoust., Speech, Signal Processing*, vol. ASSP-33, no. 3, pp. 672–683, June 1985.
[30] M. J. Vrhel and H. J. Trussell, "Filter considerations in color correction," *IEEE Trans. Image Processing*, vol. 3, no. 2, pp. 147–161, Mar. 1994.

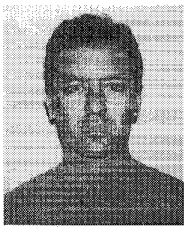

Panos E. Trahanias (M'91) received the B.Sc. degree in physics from the University of Athens, Greece, in 1985, and the Ph.D. degree in computer science from the National Technical University of Athens, Greece, in 1988.

He is an Assistant Professor in the Department of Computer Science, University of Crete, Greece, and a Senior Researcher at the Institute of Computer Science (ICS), Foundation for Research and Technology–Hellas (FORTH), Greece. From 1985 to 1989, he served as a Research Assistant at the Institute of Informatics and Telecommunications, National Center for Scientific Research "Demokritos," Athens, Greece, and from 1990 to 1991, he worked at the same Institute as a Post-Doctoral Research Associate. From 1991 to 1993, he was with the Department of Electrical and Computer Engineering, University of Toronto, Toronto, Canada, as a Post-Doctoral Research Associate. His current research interests are in the areas of computer vision and robotics, pattern recognition and image processing and analysis, as well as in systems applications of the above. He is the coordinator of the Computer Vision and Robotics Laboratory at ICS-FORTH. He has participated in many research and development programs at the University of Toronto and ICS-FORTH and has been a consultant to SPAR Aerospace Ltd., Toronto, Canada, in a program regarding the analysis of infrared images. He is member of the steering committee and coordinator of ICS-FORTH's activities in the HCM ERCIM Computer Graphics Network. He has published over 25 papers in technical journals and conference proceedings and has contributed in two books.

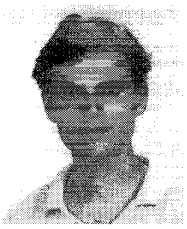

Damianos Karakos received the B.S. degree in computer science from the University of Crete, Greece, in 1995.

During his undergraduate studies, he worked as a research assistant at the Institute of Computer Science, Foundation for Research and Technology–Hellas (ICS-FORTH), Greece. Since September 1995, he has been a Ph.D. student in the Electrical Engineering Department, University of Maryland, College Park, and a research assistant at the Institute for Systems Research (ISR) in the same university. His research interests are in the areas of digital communications, information theory and signal and image processing.

Anastasios N. Venetsanopoulos (S'66–M'69 –SM'79–F'88) received the B.Eng. degree from the National Technical University of Athens (NTU), Greece, in 1965, and the M.S., M.Phil., and Ph.D. degrees in electrical engineering from Yale University, New Haven, CT, in 1966, 1968, and 1969, respectively.

He joined the University of Toronto in September 1968, where he has been a Professor in the Department of Electrical and Computer Engineering since 1981. He has served as Chairman of the Communications Group and Associate Chairman of the Department of Electrical Engineering. He was on research leave at the Federal University of Rio de Janeiro, the Imperial College of Science and Technology, the National Technical University of Athens, the Swiss Federal Institute of Technology, and the University of Florence and was an Adjunct Professor at Concordia University, Montreal, Canada. He has served as Lecturer in 130 short courses to industry and continuing education programs and as consultant to several organizations; he is a contributor to 24 books, co-author of *Nonlinear Filters in Image Processing: Principles and Applications* and *Artificial Neural Networks: Learning Algorithms, Performance Evaluation and Applications*, and has published over 500 papers on digital signal and image processing and digital communications. His present research interests include linear M-D and nonlinear filters, processing of multispectral (color) images and image sequences, telecommunications, and image compression. In particular, he has been involved with the development of efficient techniques for multispectral image transmission, restoration, filtering, and analysis.

Dr. Venetsanopoulos has served as Chairman on numerous boards, councils, and technical conference committees including IEEE committees, such as the Toronto Section (1977–1979) and the IEEE Central Canada Council (1980–1982); he was President of the Canadian Society for Electrical Engineering and Vice President of the Engineering Institute of Canada (EIC) (1983–1986). He has been a Guest Editor or Associate Editor for several IEEE journals and the Editor of the *Canadian Electrical Engineering Journal* (1981–1983). He is a member of the IEEE Communications, Circuits and Systems, Computer, and Signal Processing Societies, as well as a member of Sigma Xi, the Technical Chamber of Greece, the European Association of Signal Processing, and the Association of Professional Engineers of Ontario (APEO) and Greece. He was elected Fellow of the IEEE "for contributions to digital signal and image processing," is Fellow of the EIC and was awarded an Honorary Doctorate from the National Technical University of Athens, for his "contribution to engineering" in October 1994.